MULTIPLE DESCRIPTION CODING OF DIGITAL HOLOGRAMS USING MAXIMUM-A-POSTERIORI

Angelo Arrifano[⋆†] *Marc Antonini*[⋆] *Manuela Pereira*[†]

[⋆]I3S laboratory, University of Nice - Sophia Antipolis / CNRS, France
[†]Instituto de Telecomunicacoes, Universidade da Beira Interior, Portugal

ABSTRACT

Holography is deemed the ultimate 3D [1]. Holographic displays provide full eye accommodation, thus not causing eye strain or headaches which are an inconvenient side-effect of 3D stereo [2][3]. As the etymological meaning of Holography suggests, digital holograms store full 3D information of the recorded object (including multiple views). For that reason, storage and transmission of digital holographic video requires high bandwidth. Considering that current high-speed communication cables cannot provide enough bandwidth for the realtime transmission of holographic video, it is not unrealistic to assume that in the future the transmission of realtime holographic video might require more than one transmission channel. In that case, one can take advantage of multiple description coding (MDC) for optimally coding data between available channels and mitigate channel errors.

We present a MDC solution for transmission of holographic video from a computer host to a holographic display device using two transmission channels. To our knowledge, there are no reports of previous works regarding the MDC of digital holograms. Because digital holograms are inherently different from regular images [4], the proposed work is novel on its own. Furthermore, since the holographic format is a direct result of the physical phenomena, the holographic format will not change in the future; allowing the presented work to be a contribution for future holographic displaying technology.

Index Terms— Holography, Digital Holography, Multiple-Description-Coding, Maximum-a-Posteriori, Quantization.

1. INTRODUCTION

Holography is deemed the ultimate 3D [1]. Holographic displays provide full eye accommodation (focusing and convergence happen into the same point in the 3D space), thus not causing eye strain or headaches which are an inconvenient side-effect of 3D stereo [2][3]. It is known that current technology cannot yet provide competitive holographic displays, otherwise we (consumers) would be able to buy them. Yet, it has been possible for research groups to afford building proof-of-concept holographic recording and displaying systems which have been supporting research in the topic [5]. One of the misconceptions about holography is that it requires expensive systems and coherent light for producing digital holograms. As backed up by some research papers in the field, digital holograms can be produced, for example, from integral images [6] or 3D meshes [7].

As the etymological meaning of Holography suggests, digital holograms store full 3D information of the recorded object (including multiple views). For that reason, storage and transmission of digital holographic video requires high bandwidth. For example, the monochromatic $128\,\mathrm{bit/pixel}$ uncompressed holographic video that is being used as a basis for this paper, requires $15\,\mathrm{Gbit/s}$ of bandwidth at a standard frame rate (explained in sec. 4). Considering that, for example the latest standard of the universal serial bus (USB 3.0) can only provide $5\,\mathrm{Gbit/s}$, it is not unrealistic to assume that the realtime transmission of compressed color holographic video from a computer to a display device, might require more than one transmission channel. In that case, one can take advantage of multiple description coding (MDC) for optimally coding data between available channels and mitigate channel errors.

The MDC is a way to optimally encode and transmit data over disjoint channels, in such a way that the receiver can still decode the data from just a single channel, albeit with a loss in quality [8]. If the data from all channels is available, then the receiver can decode the data with full quality. Therefore, MDC poses as an interesting solution to avoid packet retransmission - one of the problems that hinders continuous video playback.

We present a MDC solution for transmission of holographic video from a computer host to a holographic display device using two transmission channels. To our knowledge, there are no reports of previous works regarding the MDC of digital holograms. Since digital holograms are inherently different from regular images [4], the proposed work is novel on its own. Furthermore, since the holographic format is a direct result of the physical phenomena, the holographic format will not change in the future; allowing the presented work to be a contribution for future holographic displaying technology.

The author Angelo Arrifano thanks Fundação para a Ciência e Tecnologia (FCT) for his PhD grant SFRH/BD/69710/2010.

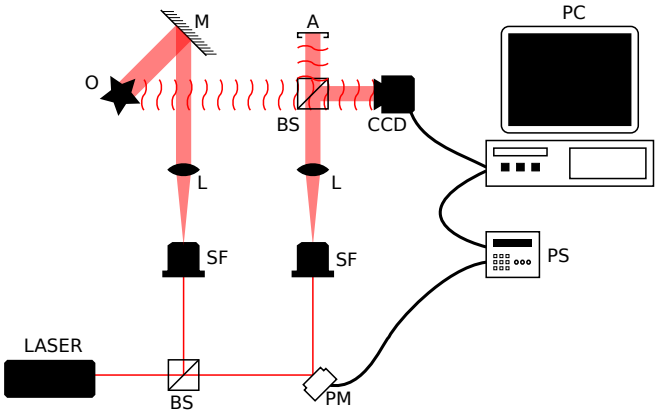

Fig. 1. The holographic recording setup: A - light absorber; BS - beam-splitter; L - collimating lens; M - mirror; O - object; PM - piezo-electric mirror; PS - power supply; SF - spatial filter.

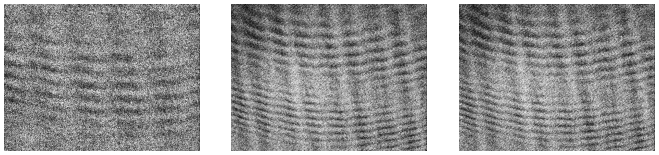

Fig. 2. Scalled hologram transmittances (amplitude only) for the "cube-v2" (first frame), "cube-v3v" and "king-v3v" sequences respectively.

2. OPTICAL RECORDING

The setup used to record digital holograms (fig. 1) follows an holographic interferometer configuration to produce in-line digital holograms. The amplitude of the wave-superposition (interference fringe) is digitized by a CMOS camera with a $2.2\,\mu\mathrm{m}$ pixel-pitch, 2592×1944 pixels of resolution and $12\,\mathrm{bit}$ of bit-depth. Because the phase information of the wave-superposition is lost during the digitizing process, one has to use the phase-shifting technique [9] to derive the amplitude+phase of the wave-superposition at the camera sensor plane. Let us refer to complex-amplitudes in this plane as the hologram transmittance from now on. The hologram transmittance $\tau(x, y)$ is calculated by recording 4 interference fringes with different phase-shifts [9]:

$$\tau = \frac{1}{4}\left(I_0 - I_\pi\right) + i\left(I_{\frac{\pi}{2}} - I_{\frac{3\pi}{2}}\right) \tag{1}$$

In fig. 2 it are shown several examples of recorded hologram transmittances, with different objects.

3. NUMERICAL RECONSTRUCTION

Having the hologram transmittance $\tau(x, y)$, one can numerically reconstruct the original object by simulating the reference light diffracting in the hologram transmittance and reassembling a complex field at the object plane, located at an distance d from the hologram plane.

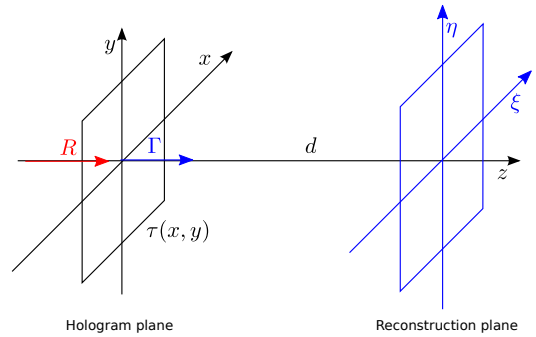

Fig. 3. Numerical hologram reconstruction: coordinate system.

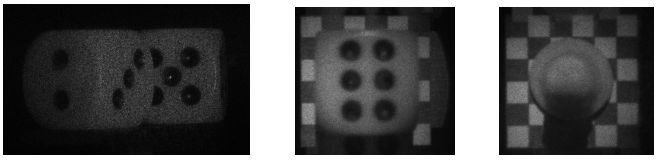

Fig. 4. Amplitude reconstructions of the "cube-v2" (first frame), "cube-v3v" and "king-v3v" holograms respectively; shown in 1:1 scale.

Consider the reference light as unitary amplitude and zero initial phase. The waves at the hologram place (fig. 3) can be propagated along the z axis into the plane ξ, η, parallel to the hologram plane, by using the Fresnel Transform [10]:

$$\Gamma(\xi, \eta) = \int\int \tau(x, y) e^{-i\pi/\lambda d(x^2+y^2)} e^{i2\pi/\lambda d(\xi x+\eta y)}\, dxdy \tag{2}$$

The previous expression can be easily discretized [10] and calculated using only one FFT [11]. The amplitude reconstruction of the object can then be obtained with:

$$I(\xi, \eta) = |\Gamma(\xi, \eta)| \tag{3}$$

In figure 4 are shown the amplitude reconstruction of several holograms. The "cube-v2" is a 39 frame sequence with 1600×1200 of pixel resolution and approximately $22.7\,\mathrm{pixels/mm}$ of spatial resolution, showing two rotating dices located at $0.245\,\mathrm{m}$ from the camera plane. The "cube-v3v" is a static (single frame) dice in front of a checkerboard and located at $0.146\,\mathrm{m}$ from the camera plane, the pixel resolution is 2592×1944 and corresponds to the maximum allowable by the camera, the spatial resolution is approximately $61.7\,\mathrm{pixels/mm}$. The "king-v3v" is similar except it shows a king piece from a chess set. All reconstructions have their speckle noise reduced by simulating temporal incoherence [12].

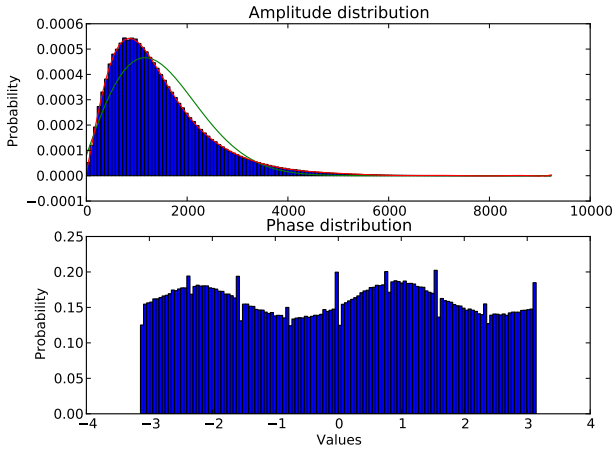

Fig. 5. Probability distribution for the amplitude and phase of a phase-shifting digital hologram.

4. THE CODING OF DIGITAL HOLOGRAMS

In the case of the aforementioned recording setup, the uncompressed storage of an hologram transmittance τ is done by saving each complex amplitude as $128\,\text{bits}$, with $64\,\text{bits}$ allocated for the real part and the other $64\,\text{bits}$ for the imaginary part, chosen to match the native type of the computer architecture. A single hologram of 2592×1944 of resolution would take approximately $644\,\text{Mbits}$ of storage space. To put this into perspective, the transmission of a $24\,\text{FPS}$ holographic video of same resolution would take $15.5\,\text{Gbits/s}$ of bandwidth. Therefore, there is a clear need of compressing the holographic video before transmission.

4.1. The information content

As reported in [4], quantization is a very effective compression mechanism for digital holograms. However, to efficiently quantize digital holograms, one must first study the nature of the information in them.

As seen previously, an hologram transmittance can be split into their amplitude A and phase ϕ representation. In fig. 5 are shown the amplitude and phase distributions of the "cube-v3v" hologram; the distributions for the other holograms are similar. With a closer look, one notices that the amplitude distribution resembles a Rayleigh distribution; indeed, there is an author that concluded exactly that [13]. However, we tried to fit a Rayleigh distribution to the sample data (fig. 5, green line) but the relative entropy between the two distributions was not convincing, this is disappointing because there are scalar quantizers optimized for Rayleigh-distributed information [14] which we could use (in the context of the next section). Nonetheless, it is clear that coding the amplitude and phase separately is better than coding them jointly.

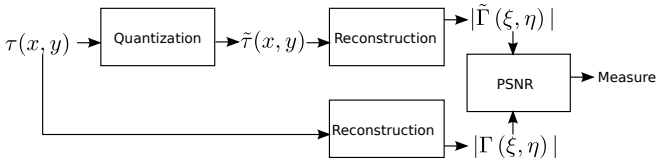

Fig. 6. Hologram quantization scheme.

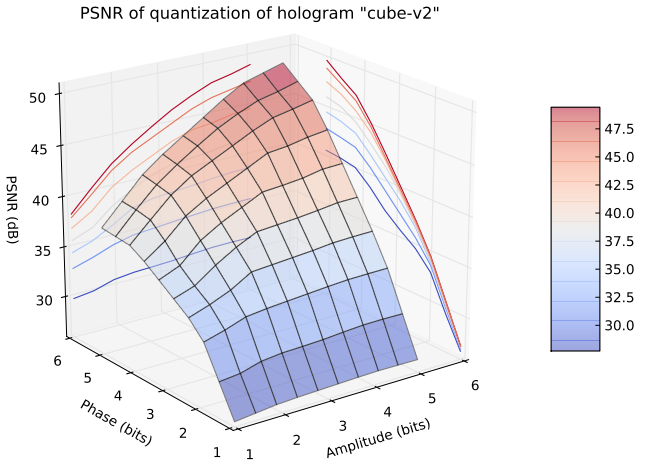

Fig. 7. Quantization of amplitude and phase of "cube-v2" sequence.

For all of our phase-shift holograms, the amplitude and phase have different probability distributions and approximately different entropies:

$$\begin{aligned} H(A) &\approx 13\,\text{bits} \\ H(\phi) &\approx 17\,\text{bits} \end{aligned}$$

4.2. Quantization

Consider fig. 6 which shows a scheme for measuring the efficiency of scalar quantization on digital holograms. The optimal quantization codebook is obtained by means of the k-means algorithm. The intensities reconstruction $|\tilde{\Gamma}(\xi,\eta)|$ of the quantized hologram transmittance is compared with the uncompressed intensities reconstruction by means of the PSNR measure. In figure 7 is shown the mean PSNR value for several quantization levels on amplitude and phase, for the "cube-v2" hologram. Notwithstanding, the PSNR curves are similar for other hologram sequences. Notice that using more than 2^6 levels provides little benefits on quality. It is also clear that the phase information contributes more to the quality of reconstruction than amplitude information, with amplitude providing little improvement on quality for a low fidelity of phase.

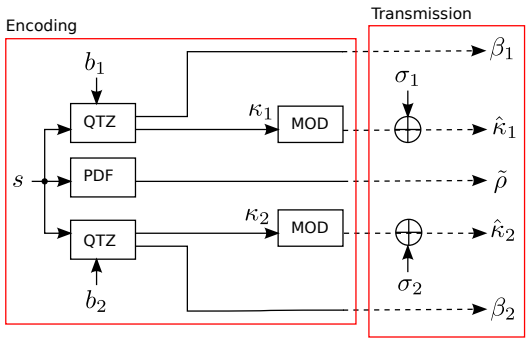

Fig. 8. Multiple description (enc)coding scheme.

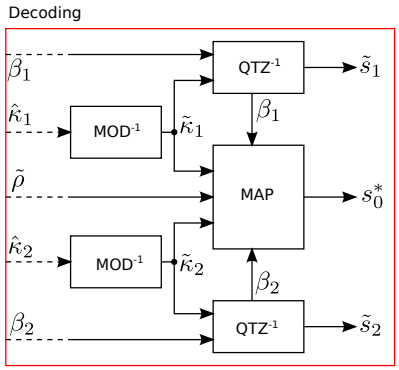

Fig. 9. Multiple description (de)coding scheme.

4.3. Encoding multiple descriptions using quantization

Consider figure 8 which depicts a scheme for encoding digital holograms into multiple descriptions. The scheme is applied independently for the amplitude A and phase ϕ of the hologram transmittance, since it was seen in section 4.1 that it is more efficient to code them separately. In this scheme, the probability density distribution of the source s (either the amplitude A or phase ϕ) is first calculated, the resulting distribution $\tilde{\rho}$ consisting of $N_\kappa$bins is transmitted to the source over a noiseless channel. The source s is then copied into two similar descriptions. Each description d is scalar quantized with the quantization codebook β_d, generated using the k-means algorithm, to produce a collection of indexes κ_d. The number of symbols in the codebook is 2^{b_d}, with b_d being inputted as a parameter to the coding system. The codebook is then transmitted to the receiver through a noiseless channel; while the indexes κ_d are modulated using binary phase-shift keying (BPSK) and transmitted to the receiver over a channel with additive white Gaussian noise (AWGN), with variance σ_d.

4.4. Decoding multiple descriptions using MAP

At the receiver, the decoder is inputted with the source probability distribution $\tilde{\rho}$ and the two descriptions, each containing the modulated quantization indexes $\hat{\kappa}_d$ and the respective codebook β_d. Without any prior information on the channel, one can only demodulate (hard decision) the quantization indices and use the codebook to recover a noisy representation of the source $\tilde{s_d}$. However, since there is prior information on the channel (σ_d) and on the distribution of the source ($\tilde{\rho}$), one can use a maximum-a-posteriori estimator (MAP) to recover an higher fidelity representation of the source (s_0^*) [15] [16].

The maximization problem can be seen as [15]:

$$(s_1^*, s_2^*) = arg \max_{s_1,s_2} p(s_1, s_2|\tilde{s}_1, \tilde{s}_2) \tag{4}$$

where s_d is a quantized symbol at the emitter. Further solving using Bayes theorem leads to

$$(s_1^*, s_2^*) = arg \min_{s_1,s_2} -log[p(s_1, s_2)p(\tilde{s}_1|s_1)p(\tilde{s}_2|s_2)] \tag{5}$$

The joint-probability in the equation is calculated with [15]:

$$p(s_1, s_2) = \int_{\max(s_1-\frac{q_1}{2}, s_2-\frac{q_2}{2})}^{\min(s_1+\frac{q_1}{2}, s_2+\frac{q_2}{2})} \tilde{\rho}(x)\, dx \tag{6}$$

where q_1, q_2 are the quantization steps for description 1 and 2 respectively.

The minimization of equation 5 leads to the estimation of the optimal side description coefficients s_1^* and s_2^*. The decision to select s_1^* or s_2^* for estimating s_0^* is based on the calculation of the quantization distortions D_1 and D_2 and then choosing the lowest D_d [15]:

$$D_d = \sum_{s_d \in \beta_d} p(\tilde{s}_d|s_d) \int_{s_d^*-\frac{q_d}{2}}^{s_d^*+\frac{q_d}{2}} (x - s_d^*)^2 \tilde{\rho}(x)\, dx \tag{7}$$

To compute equation 5 one also needs to calculate the transition probability $p(\tilde{s}_d|s_d)$ for channel d. In this case, the channel noise distribution corresponds to a zero-mean additive white Gaussian noise (AWGN) with variance σ_d^2:

$$p(\tilde{s}_d|s_d) = \frac{1}{\sqrt{(2\pi\sigma_d^2)^M}} exp\left(-\frac{|\tilde{\kappa}_d - u(s_d)|^2}{2\sigma_d^2}\right) \tag{8}$$

where $u(s)$ is a function that represents the symbol s after quantization and modulation.

5. RESULTS

The coding process described in section 4, was applied to the amplitude and phase of the holograms transmittances presented in section 2. The output of the coding process is $\tilde{A}_1, \tilde{A}_2, A_0^*$ and $\tilde{\phi}_1, \tilde{\phi}_2, \phi_0^*$ which can be assembled with $\tau = Ae^{i\phi}$ to produce $\tilde{\tau}_1, \tilde{\tau}_2, \tau_0^*$, corresponding to the hard-decoded and the MAP-decoded hologram transmittances. Afterwards, each of the hologram transmittances is wave-propagated at a distance d using the Fresnel transform (section 3), to obtain the complex amplitudes at the object plane.

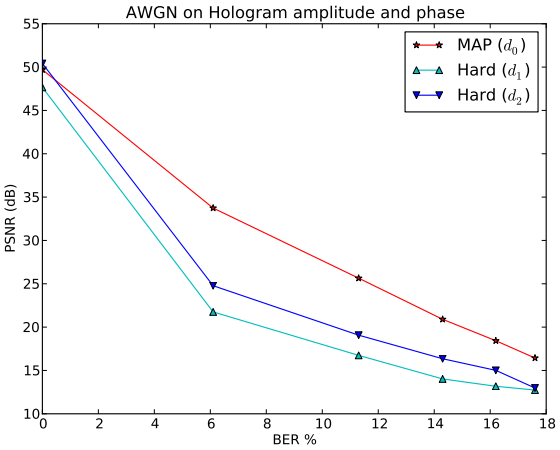

Fig. 10. MDC of the "cube-v3v" hologram; using $b_1 = 5, b_2 = 6$ bits for quantization; $\sigma_2 = 0.8 \times \sigma_1$.

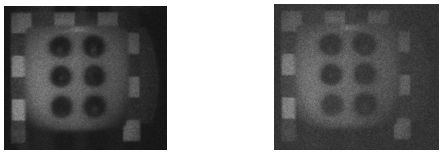

Fig. 11. Intensity reconstructions of the "cube-v3v" hologram, for a BER$\approx$ 11.5 %. MAP-decoding (left) and hard-decision (right).

The wave propagation is performed several times with different wavelengths, as to simulate temporal incoherence and therefore reducing speckle noise [12]. Finally, the intensities reconstruction from each of the holograms transmittances is obtained by using eq. 3. The reconstructed intensities $\tilde{I}_1, \tilde{I}_2, I_0^*$, can be compared with an uncompressed and noiseless intensity I by using the PSNR measure (see fig. 6). Please remark that this is only possible because the speckle of the images was reduced using the technique in [12].

Consider fig. 10 which shows the PSNR of the reconstructed intensities of hologram "cube-v3v" using hard-decision and MAP, for several channel errors. The AWGN variance of channel 2 is always 80 % of the variance of channel 1. The hologram transmittance was quantized with 10 bits for description 1 and 12 bits for description 2, being the bits split equally between the amplitude and phase. As we can see, the MAP decoding provides between 2 dB and 10 dB and of quality improvement upon varying channel noise. It is also interesting to refer that holograms alone are also very robust to AWGN (fig. 10). Regular 2D images subject to the same levels of quantization and white noise, would not provide 14 dB of quality for a bit-error-rate (BER) as high as 18 %. In figures 11 and 12 we can see a comparison between the intensities reconstruction using hard-decision and

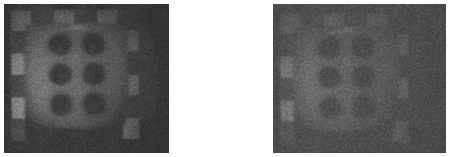

Fig. 12. Intensity reconstructions of the "cube-v3v" hologram, for a BER$\approx$ 17.8 %. MAP-decoding (left) and hard-decision (right).

the MAP-decoder. It is clear the MAP algorithm provides better quality, also notice that an additive white noise in the hologram transmittance directly translates into an increase of speckle noise in the intensities reconstruction.

6. CONCLUSION

In this paper it was seen that scalar quantization is an effective tool for digital hologram compression, which meets the study presented in [4]. If one-dimensional quantization is an effective compression tool for digital holograms, what about vector quantization? Vector quantization allows the exploitation of multi-dimensional spatial correlation providing an increased coding efficiency.

It was also seen that MDC is a powerful mechanism to mitigate channel errors on digital holograms. Nonetheless, fig. 7 provides good insight about the independent contribution that amplitude and phase have on the reconstruction, possibly leading to an optimal bit-allocation scheme for the MDC of digital holograms.

To our knowledge, this is the first study about MDC of digital holograms. For this reason, we hope on giving a valuable contribution and stimulate further research in the source and channel coding communities.

7. ACKNOWLEDGMENTS

The authors would like to thank to the professor Paulo T. Fiadeiro from the "Unidade de Detecção Remota e Centro de Óptica, Universidade da Beira Interior, Portugal" for his valuable time and expertise on building the holographic setup referred in section 2.

8. REFERENCES

[1] L. Onural, "Television in 3-D: What are the prospects?," *Proceedings of the IEEE*, vol. 95, no. 6, pp. 1143–1145, 2007.

[2] J. S. McVeigh, M. W. Siegel, and A. G. Jordan, "Algorithm for automated eye strain reduction in real stereoscopic images and sequences," *SPIE Human Vision and Electronic Imaging*, vol. 2657, pp. 307–316, 1996.

[3] A. Smolic, "3D video and free viewpoint video - From capture to display," *Elsevier Pattern Recognition*, vol. 44, no. 9, pp. 1958–1968, Sept. 2011.

[4] T. J. Naughton, Y. Frauel, B. Javidi, and E. Tajahuerce, "Compression of digital holograms for three-dimensional object reconstruction and recognition," *Applied Optics*, vol. 41, no. 20, pp. 4124–32, July 2002.

[5] D. P. Kelly, D. S. Monaghan, N. Pandey, T. Kozacki, A. Michalkiewicz, G. Finke, B. M. Hennelly, and M. Kujawinska, "Digital Holographic Capture and Optoelectronic Reconstruction for 3D Displays," *International Journal of Digital Multimedia Broadcasting*, vol. 2010, pp. 1–14, 2010.

[6] T. Mishina, M. Okui, and F. Okano, "Calculation of holograms from elemental images captured by integral photography," *Applied Optics*, vol. 45, no. 17, pp. 4026–4036, 2006.

[7] K. Matsushima and S. Nakahara, "Extremely high-definition full-parallax computer-generated hologram created by the polygon-based method.," *Applied optics*, vol. 48, no. 34, pp. H54–63, Dec. 2009.

[8] V. K. Goyal, "Multiple description coding: Compression meets the network," *IEEE Signal Processing Magazine*, vol. 18, no. 5, pp. 74–93, 2001.

[9] I. Yamaguchi and T. Zhang, "Phase-shifting digital holography," *Optics Letters*, vol. 22, no. 16, pp. 1268–70, Aug. 1997.

[10] U. Schnars and W. Jüptner, "Digital recording and numerical reconstruction of holograms," *Measurement Science and Technology*, vol. 13, no. 9, pp. 4812–20, Aug. 2002.

[11] U. Schnars and W. Jüptner, "Direct recording of holograms by a CCD target and numerical reconstruction.," *Applied optics*, vol. 33, no. 2, pp. 179–81, Jan. 1994.

[12] B. M. Hennelly, D. P. Kelly, J. Maycock, T. J. Naughton, and J.B. McDonald, "Speckle Reduction from Digital Holograms by Simulating Temporal Incoherence," *Proceedings of the SPIE*, vol. 6696, pp. 66961I–12, 2007.

[13] E. Buckley, "Holographic laser projection," *IEEE Journal of Display Technology*, vol. 7, no. 3, pp. 135–140, 2011.

[14] W. Pearlman and G. Senge, "Optimal quantization of the Rayleigh probability distribution," *IEEE Transactions on Communications*, vol. 27, no. 1, pp. 101–112, Jan. 1979.

[15] M. A. Agostini and M. Antonini, "Multiple description video decoding using MAP," *IEEE International Conference on Image Processing*, pp. 1228–1231, 2008.

[16] A. Arrifano, M. Antonini, M. Pereira, and M. M. Freire, "Joint source-channel decoding of motion-information using maximum-a-posteriori," *IEEE International Conference on Image Processing*, pp. 2221–2224, 2011.